Notes on Numerical Fluid Mechanics
and Multidisciplinary Design 136

Andreas Dillmann
Gerd Heller
Ewald Krämer
Claus Wagner
Stephan Bansmer
Rolf Radespiel
Richard Semaan *Editors*

New Results in Numerical and Experimental Fluid Mechanics XI

Contributions to the 20th STAB/DGLR Symposium Braunschweig, Germany, 2016

Springer

Notes on Numerical Fluid Mechanics and Multidisciplinary Design

Volume 136

Notes on Numerical Fluid Mechanics and Multidisciplinary Design publishes state-of-art methods (including high performance methods) for numerical fluid mechanics, numerical simulation and multidisciplinary design optimization. The series includes proceedings of specialized conferences and workshops, as well as relevant project reports and monographs.

More information about this series at http://www.springer.com/series/4629

Andreas Dillmann · Gerd Heller
Ewald Krämer · Claus Wagner
Stephan Bansmer · Rolf Radespiel
Richard Semaan
Editors

New Results in Numerical and Experimental Fluid Mechanics XI

Contributions to the 20th STAB/DGLR Symposium Braunschweig, Germany, 2016

Springer

Editors
Andreas Dillmann
Institut für Aerodynamik und Strömungstechnik
Deutsches Zentrum für Luft- und Raumfahrt
Göttingen
Germany

Gerd Heller
Airbus Deutschland
Bremen
Germany

Ewald Krämer
Institut für Aerodynamik und Gasdynamik
Universität Stuttgart
Stuttgart
Germany

Claus Wagner
Institut für Aerodynamik und Strömungstechnik
Deutsches Zentrum für Luft- und Raumfahrt
Göttingen
Germany

Stephan Bansmer
Institut für Strömungsmechanik
Technische Universität Braunschweig
Braunschweig
Germany

Rolf Radespiel
Institut für Strömungsmechanik
Technische Universität Braunschweig
Braunschweig
Germany

Richard Semaan
Institut für Strömungsmechanik
Technische Universität Braunschweig
Braunschweig
Germany

ISSN 1612-2909 ISSN 1860-0824 (electronic)
Notes on Numerical Fluid Mechanics and Multidisciplinary Design
ISBN 978-3-319-64518-6 ISBN 978-3-319-64519-3 (eBook)
https://doi.org/10.1007/978-3-319-64519-3

Library of Congress Control Number: 2017948215

Printed on acid-free paper

This Springer imprint is published by Springer Nature
The registered company is Springer International Publishing AG
The registered company address is: Gewerbestrasse 11, 6330 Cham, Switzerland

Preface

This volume contains the papers presented at the 20th DGLR/STAB-Symposium held in Braunschweig, Germany (November 8–9, 2016), organized by the Institute of Fluid Mechanics of the Technische Universität Braunschweig. STAB is the German Aerospace Aerodynamics Association (Deutsche Strömungsmechanische Arbeitsgemeinschaft) founded towards the end of the 1970s, whereas DGLR is the German Society for Aeronautics and Astronautics (Deutsche Gesellschaft für Luft- und Raumfahrt - Lilienthal Oberth e.V.).

The mission of STAB is to foster aerodynamics research and its appreciation in Germany. This is accomplished by creating vivid forums for scientific discussions and by disseminating most recent research results, thereby enhancing scientific progress and avoiding unnecessary duplication in research work. Particularly today, this is more crucial than ever. Thanks to the experience and methodologies gained in the past, it is now easier to obtain new knowledge for solving today's and tomorrow's problems. STAB unites German scientists and engineers from universities, research establishments and the industry, involved in research and project work in the field of numerical and experimental fluid mechanics and aerodynamics for aerospace, ground transportation and other applications. This is a solid basis for numerous common research activities sponsored by different funding agencies.

Since 1986, the symposium has taken place at different locations in Germany every two years. In between, STAB workshops have been held regularly at the DLR in Göttingen. The various symposia locations across Germany represent focal points in Germany's Aerospace Fluid Mechanics Community. The STAB symposia and workshops provide excellent forums where new research activities can be presented, often resulting in new jointly organized research and technology projects.

It is the eleventh time that the contributions to the symposium are published after being subjected to a peer review. The present contributions highlight the current key area of integrated research and development based on the fruitful collaboration of industry, research establishments and universities. The research areas include

airplane and ground vehicle aerodynamics, multidisciplinary optimization and new configurations, turbulence research and modelling, laminar flow control and transition, rotorcraft aerodynamics, aeroelasticity and structural dynamics, numerical and experimental simulation including test techniques, aeroacoustics as well as biomedical and convective flows.

From some 77 lectures presented at the symposium, 67 are included in this book.

The review board, partly identical with the programme committee, consisted of:

K. Backhaus (Braunschweig), P. Bahavar (Göttingen), G. Bangga (Stuttgart), S. Bansmer (Braunschweig), H. Barth (Göttingen), C. Bauer (Göttingen), A. Bauknecht (Göttingen), T. Berkefeld (Göttingen), P. Bernicke (Braunschweig), A. Berthold (Berlin), J. Braukmann (Göttingen), M. Braune (Göttingen), C. Breitsamter (München), D. Burzynski (Braunschweig), A. Buzica (München), L. Capsada (Braunschweig), J. Delfs (Braunschweig), F. Edzards (Göttingen), T. Eggers (Braunschweig), K. Ehrenfried (Göttingen), R. Ewert (Braunschweig), N. Fehn (München), M. Fehrs (Göttingen), A. Feldhusen-Hoffmann (Aachen), D. Feldmann (Göttingen), U. Fey (Göttingen), A. Fischer (Stuttgart), H. Foysi (Siegen), A. Gardner (Göttingen), R. Geisler (Göttingen), A. Goerttler (Göttingen), J. Haff (Göttingen), F. Haucke (Berlin), S. Haxter (Göttingen), A. Heider (Göttingen), S. Hein (Göttingen), R. Heinrich (Braunschweig), H. Heißelmann (Oldenburg), C. Heister (Braunschweig), A. Henning (Göttingen), M. Herr (Braunschweig), E. Jost (Stuttgart), T. Kächele (München), S. Keye (Braunschweig), C. Kiefer (Saarbrücken), M. Klaas (Aachen), C. Klein (Göttingen), T. Knopp (Göttingen), F. Knoth (München), S. Koch (Göttingen), M. Konstantinov (Göttingen), T. Köthe (Göttingen), M. Kronbichler (München), A. Krumbein (Göttingen), M. Kruse (Braunschweig), A. Kümmel (München), K. Kutscher (Braunschweig), T. Landa (Braunschweig), P. Lehmann (Braunschweig), J. Lohse (Berlin), H. Lüdeke (Braunschweig), J. Lunte (Göttingen), T. Lutz (Stuttgart), P. Marquardt (Aachen), J. Martinez Schramm (Göttingen), R. Meyer (Göttingen), F. Muñoz (Braunschweig), J. Neumann (Göttingen), J. Piquee (München), A. Probst (Göttingen), S. Probst (Göttingen), D. Puckert (Stuttgart), M. Raffel (Göttingen), M. Rein (Göttingen), J. Reiss (Berlin), A. Rempke (Braunschweig), M. Ripepi (Braunschweig), U. Rist (Stuttgart), H. Rosemann (Göttingen), M. Rütten (Göttingen), L. Savoni (Braunschweig), D. Schiepel (Göttingen), T. Schneider (München), C. Schnepf (Göttingen), G. Schrauf (Bremen), A. Schröder (Göttingen), E. Schülein (Göttingen), D. Schütz (Siegen), D. Schwamborn (Göttingen), R. Semaan (Braunschweig), A. Shishkin (Göttingen), L. Siegel (Göttingen), M. Staats (Berlin), L. Stein (Berlin), C. Stemmer (München), M. Stuhlpfarrer (München), C. Voß (Göttingen), C. Wagner (Göttingen), A. Waldmann (Stuttgart), P. Weihing (Stuttgart), K. Weinman (Göttingen), S. Weiss (Göttingen), A. Westhoff (Göttingen), T. Wetzel (Göttingen), S. Wiggen (Göttingen), H. Wilhelmi (Göttingen), M. Winter (München), C. Wolf (Göttingen), J. Zahn (Stuttgart).

Nevertheless, the authors are responsible for the contents of their contributions.

The editors are grateful to Prof. Dr. W. Schröder as the General Editor of the "Notes on Numerical Fluid Mechanics and Multidisciplinary Design" series and to the Springer publishing house for the opportunity to publish the results of the symposium.

Göttingen, Germany — Andreas Dillmann
Bremen, Germany — Gerd Heller
Stuttgart, Germany — Ewald Krämer
Göttingen, Germany — Claus Wagner
Braunschweig, Germany — Rolf Radespiel
Braunschweig, Germany — Stephan Bansmer
Braunschweig, Germany — Richard Semaan
April 2017

Contents

Part I
Airplane Aerodynamics/Propulsion Integration

Numerical Investigation of Slot and Configuration Impact on the Efficiency of Tangential Blowing at a Vertical Tailplane with Infinite Span

Anna Gebhardt and Jochen Kirz

Abstract On a swept vertical tailplane with infinite span tangential blowing over the shoulder of a deflected rudder is applied. For large rudder deflection angles the flow on the rudder is separated without blowing. A numerical study is conducted with the aim to increase the side force coefficient which might be required for a take-off condition if a one-sided engine failure occurs. With a continuous slot and sufficient mass flow rate the separation on the rudder can be reduced or avoided. It is shown that by using discrete slots this can be achieved for a similar side force coefficient gain with a smaller momentum coefficient. In addition the sweep angle of the incoming flow is varied showing a strong impact on the achievable side force coefficient. This is also true for the curvature of the rudder shoulder over which the jet is blown.

1 Introduction

The vertical tailplane (VTP) of a transport aircraft is needed for stability and control of the aircraft about the yaw axis. One important sizing case of the VTP for modern aircraft is an one engine inoperative (OEI) condition with the failure of the critical engine. In this situation an asymmetric thrust is created. The resulting moment around the yaw axis must be counteracted by the VTP. Here take-off is a critical flight segment where high thrust requirements lead to a high yawing moment which necessitates large aerodynamic forces to be generated by the VTP. On the other hand the flight speed is relatively low leading to relatively low aerodynamic forces produced by the VTP demanding a large size. However, in cruise flight at high aircraft velocity, the VTP is larger than necessary to satisfy cruise stability requirements for

A. Gebhardt (✉) · J. Kirz
DLR (German Aerospace Center), Institute of Aerodynamics and Flow Technology, Transport Aircraft, Lilienthalplatz 7, 38108 Braunschweig, Germany
e-mail: anna.gebhardt@dlr.de

J. Kirz
e-mail: jochen.kirz@dlr.de

A. Dillmann et al. (eds.), *New Results in Numerical and Experimental Fluid Mechanics XI*, Notes on Numerical Fluid Mechanics and Multidisciplinary Design 136, https://doi.org/10.1007/978-3-319-64519-3_1

modern transport aircraft with electronic flight control systems. It follows that the VTP size is determined by a rarely occurring failure case. In this critical OEI case the rudder is highly deflected to achieve maximum side force but this also leads to partial separation on the rudder. If the size of the VTP could be reduced by applying some means to increase the side force, drag and weight could be lowered which in turn would lead to a reduction in fuel burn. One possibility is the use of active flow control (AFC). With this the side force coefficient C_Y produced by the VTP can be increased without increasing its size by delaying flow separation to higher sideslip and/or rudder deflection angles.

In contrast to passive flow control using for example vortex generators, active flow control has the possibility to be turned on just when needed. On the other hand some source of energy is needed for the AFC system which is not the case for a passive system. For this investigation, pressurized air is used as the energy source to drive fluidic actuators. These are already used in a wide range of active flow control applications. Among different kinds of blowing techniques tangential blowing over the rudder is selected for the current study.

Sensitivities of different active flow control parameters were investigated in a previous study using a 2D VTP airfoil [5]. The results showed that the flow on the rudder can remain attached on the rudder also at high deflection angles if the blowing velocity and mass flow rate are sufficiently high. This was accompanied by an increase of the lift coefficient of the airfoil. Tangential blowing has already been investigated experimentally and numerically in several studies, e.g. [1, 8], but mainly for the use on wings. Due to the small aspect ratio and the large sweep angle of the VTP the results obtained for the wing might not be directly transferable. Recently research was done at NASA and Boeing with a VTP geometry using an experimental approach [6] subsequently supported by numerical results. However, for these studies different kinds of actuators were used, namely synthetic jets and sweeping jets, what might lead to a different interaction with the flow field. In addition, no study was found in which the underlying mechanism driving the variable efficiency of different slot configurations along the VTP span was investigated.

In the frame of the current study the numerical investigation to increase the side force coefficient by tangential blowing is extended to 3D. This allows examining effects in spanwise direction. Here the width of discrete slots and the size of the gap between them are varied as well as the blowing velocity. In this study, starting from a continuous jet, the slot area is reduced in spanwise direction. Since a whole 3D VTP would mean a large mesh resulting in excessive calculation time, a 2.5D geometry is used. It has an infinite span and a constant chord length but incorporates the sweep angle of the VTP. In addition to a variation of the slots the leading edge sweep angle is also altered since it is expected to have an impact on the side force increase at a constant momentum coefficient. In addition a variation of the curvature of the rudder shoulder just behind the blowing slots is examined.

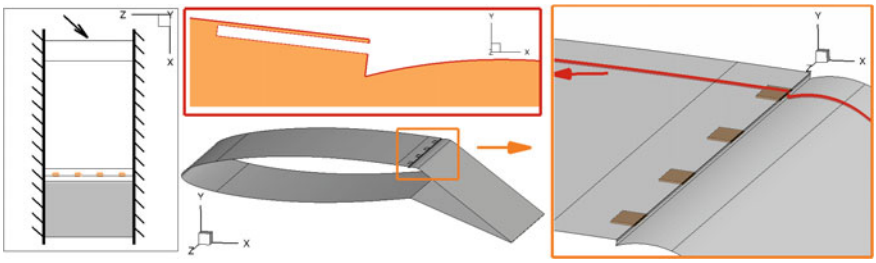

Fig. 1 Overview of geometry: *Left* Top view of VTP section with periodic boundaries *left* and *right*; middle bottom: side aft view of VTP section; *right* detail view of slots and rudder shoulder; *middle top* slice through one slot and rudder shoulder

2 Geometry

The VTP section considered consists of a symmetrical airfoil which is constant over the span. Selected is the NACA 63A010 which is a transonic airfoil suited for a conventional transport aircraft. The hinge-line, separating the non-moving part fin and the deflectable rudder, is situated at 67% chord length. Since this is a 2.5D approach, the chord length is kept constant over the span. The sweep angle is about 44°, which is similar to the sweep angle of a VTP leading edge. It is varied for an investigation of the sweep angle influence on the results. The rudder deflection angle of about 23° in direction of the incoming flow is selected due to the occurrence of notable flow separation for these conditions. The side slip angle is zero for all investigations. The geometry is scaled by about 1:11 to correspond to a wind tunnel scale and to make the results more easily comparable with other studies.

In the geometry a slot is integrated at the end of the fin as shown in Fig. 1 to allow for tangential blowing. The slot height is 0.06% of the chord length leading to a relatively thin slot. This height was also used for the preceding 2D investigations [5]. A part of the slot is modelled for numerical reasons [3]. The slot length corresponds to 20 times the slot height and is chosen so that a developed pipe flow is established at the outlet. A small step is located aft of the slot towards the rudder shoulder, which would be expected for a realistic 3D design as well, if only due to material thickness.

At first a geometry with a continuous slot is used. In a next step several discrete slots are introduced in spanwise direction. The span is kept constant for the investigation and the width of the actuators is selected to fit this span. Just a limited spanwise section is calculated. The left and right boundaries of this section are set as periodic boundaries, resulting in a simulation of an infinite swept wing-type geometry.

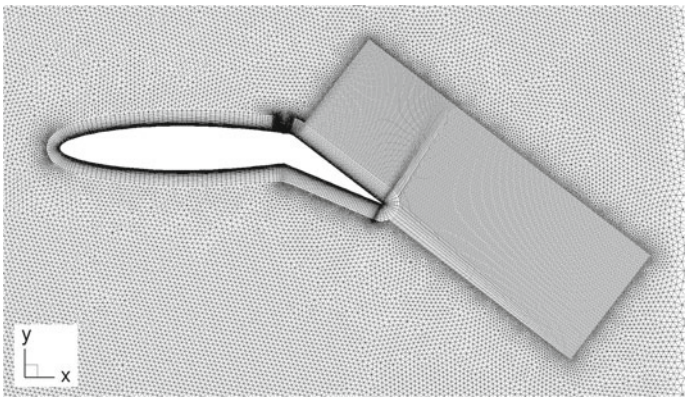

Fig. 2 Slice of the mesh showing the hexahedron blocks used for field refinement

3 Mesh Generation

Hybrid grids are created with the commercial mesh generation package CENTAUR from CentaurSoft [2]. The mesh consists in the near wall region of hexahedrons on most parts of the rudder and on the remaining parts of prisms. For the field refinement above and behind the rudder hexahedrons are used as well. These are directly connected to the near wall mesh above the rudder and at its trailing edge. This approach should lead to improved capturing and preservation of the flow quantities compared to a mesh using prisms and/or tetrahedra instead. The slot is meshed as far as possible in a structured way. The remainder of the flow field is filled with tetrahedrons. Some aspects of mesh dependence were studied in a preliminary investigation described in [5] for a 2D case. The farfield extends 100 times the VTP chord length in x- and y-direction. The overall number of points is about 7 million by using 50 prism layers and a target $y^+ = 0.5$. An overview of the mesh in the vicinity of the geometry is presented in Fig. 2.

4 Flow Simulation

The flow computations were carried out with the flow solver TAU, release 2015.1.0, developed by DLR (Deutsches Zentrum für Luft- und Raumfahrt, German Aerospace Center) [4]. The TAU software solves the Reynolds-averaged Navier-Stokes (RANS) equations using numerical methods in two or three dimensions on unstructured and hybrid grids. For the spatial discretization a finite volume method is applied.

The temporal discretization is realized by a semi-implicit Backward-Euler scheme with the linear LUSGS (Lower-Upper Symmetric Gauss-Seidel) solver. A matrix dissipation scheme is employed for low numerical dissipation. The Reynolds number

is $Re = 2.24 \cdot 10^6$ for the VTP chord length in direction of the incoming flow at a Mach number of $M_\infty = 0.2$ or a flow velocity of $v_\infty = 69\,\mathrm{m/s}$.

The steady, viscous, fully turbulent RANS calculations were performed using the turbulence model of Spalart and Allmaras [10] enhanced with a vortical and rotational flow correction (SARC) based on the approach of Spalart-Shur [9]. For circulation control airfoils it was shown that this turbulence model leads to good results for flows with high streamline curvature [7].

For the calculations with blowing activated, an actuation boundary condition is specified at the upstream wall of the slot to inject the jet flow into the flow domain. For this boundary condition a specification of jet velocity and density is necessary, with the latter assumed to be identical to the value of the flow in the farfield.

When comparing the results of the flow simulations, the dimensionless momentum coefficient C_μ is used. It is defined as:

$$C_\mu = \frac{\dot{m}_j \cdot v_j}{\frac{1}{2} \cdot \rho_\infty \cdot v_\infty^2 \cdot A_{\mathrm{ref}}} = \frac{v_j^2 \cdot \rho_j \cdot A_j}{\frac{1}{2} \cdot \rho_\infty \cdot v_\infty^2 \cdot A_{\mathrm{ref}}} \tag{1}$$

where $\dot{m}_j$ is the mass flow rate of the jet through the actuator slot with the jet velocity v_j and the jet density ρ_j. The variables ρ_∞ and v_∞ are the density and velocity of the onset flow in the farfield, A_j is the accumulated area of the slot exit and A_{ref} is the reference area of the model used, which is the chord length times the span.

5 Results

This section begins with the presentation of the results of the slot variations. Thereafter the results of the variation of the sweep angle are shown followed by the variation of the rudder shoulder curvature.

5.1 Variations of Slot Width and Gap Size

First, calculations are done using a continuous slot extending over the whole span. Without blowing activated the rudder is separated. Increasing the jet velocity or momentum coefficient the separation over the rudder is reduced. This leads, as shown in Fig. 3, to an increase of the side force coefficient which is here given as an increment to the case without blowing. The force coefficients are obtained by integration of the surface pressure and friction drag excluding the jet boundary plane. The jet adds energy close to the rudder surface. Due to this the flow can better sustain the adverse pressure gradient further downstream on the rudder. Beyond $C_\mu = 1\%$ the flow is fully attached up to the rudder trailing edge. C_Y, which is defined as

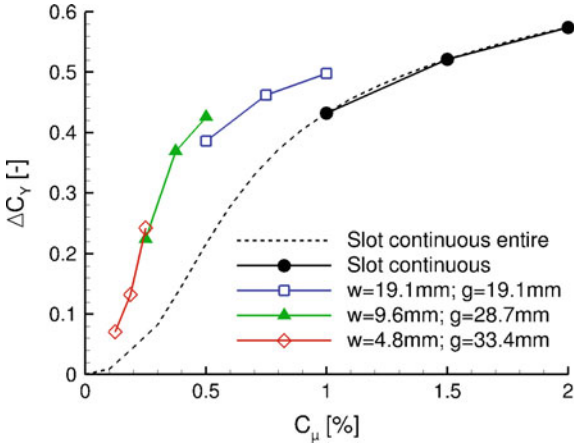

Fig. 3 C_Y increment versus C_μ for different slot width w and gap size g for a number of slots of 4 compared to the continuous slot, each row shows results for 3 different jet velocities

$C_Y = {}^{Y}/_{\frac{1}{2}\cdot\rho_\infty\cdot v_\infty^2\cdot A_{\text{ref}}}$ with Y being the side force, increases further but the efficiency of the blowing reduces. For the same amount of C_μ a smaller increase in C_Y is obtained.

In a next step the continuous slot is replaced by four discrete slots. Their width and gap size is varied. The effect on C_Y is shown in Fig. 3. For each data row being a gap/width combination three different jet velocities are calculated. The three jet velocities v_j are: 169 m/s, 207 m/s, and 239 m/s. The smallest jet velocity leads thereby to the smallest C_μ in a data row. For the continuous slot the dashed line gives additional results.

As can be seen, side force coefficients similar to the lowest of the three points of the continuous slot can be obtained for some of the discrete slot configurations at a lower C_μ. For the geometry with $w = 9.6$ mm this would correspond to the third point in its row which is obtained using the highest jet velocity of 239 m/s. The jet velocity is increased compared to the continuous slot but the jet exit area is greatly reduced leading to the reduction in C_μ of 50% and a reduction in the mass flow rate of about 65% for nearly the same side force coefficient.

This can be explained by the vortex system which develops over the rudder when using the discrete slots. An example is shown in Fig. 4. Two effects are responsible for this. Due to the finite length of the discrete slots the jets have edges left and right. In addition, the incoming flow has an angle to the blowing direction of the jets which is at the slot exit perpendicular to the hinge-line. The shearing of the incoming flow with the jets leads to the generation of a counter-rotating vortex pair at each jet. When looking from behind at the rudder the right vortex of each pair is rotating clockwise having a negative ω_x which is the sense of rotation in x-direction. The left vortex is rotating counter-clockwise. In the middle of a vortex pair an upwind region is created which is locally disadvantageous since it transports fluid away from the surface. At the other sides of the vortex pair the vortices are rotating downwards to the surface enhancing the mixing of the outer flow with the boundary layer. This has a favorable impact helping to attach the flow to the rudder in the areas between the jets. The

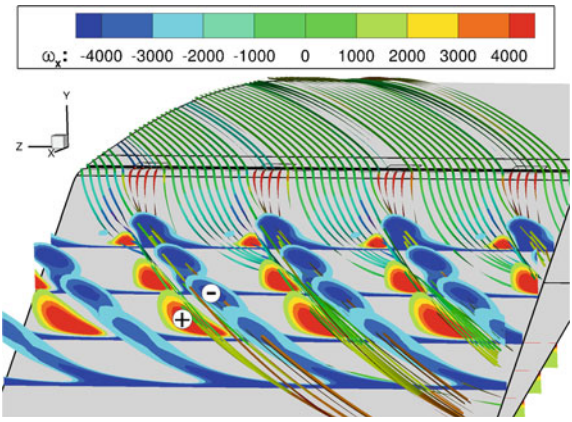

Fig. 4 Rear view onto the rudder: field stream traces and vortices generated by 4 discrete slots ($w = 9.6$ mm, $v_j = 207$ m/s)

generation of the vortices and their efficiency is dependend on the slot width and gap size as well as on the jet velocity. With increasing jet velocity the energy added to the flow is increased and the jet blowing direction becomes more dominant further downstream on the rudder while for low jet velocities the incoming flow turns the jet in its direction.

For the smallest slot width $w = 4.8$ mm in Fig. 3 the slot area is quite small as is thus the momentum coefficient. So altogether not enough energy is added to the flow over the rudder to attach it up to the trailing edge. Increasing C_μ by increasing the slot width extends the areas of attached flow on the rudder and thus the side force coefficient. The largest slot width of the discrete slots tends towards the results of the continuous slots. However, since the slot area and C_μ is still smaller only the continuous slot can reach the maximum side force calculated.

5.2 Variation of the Sweep Angle

In this study an infinite section with constant chord and constant sweep angle for the leading and trailing edge and the hinge-line is used. For the real 3D VTP the planform is tapered with a large chord length at the root and a smaller one at the tip. This leads usually to a hinge-line sweep angle which is smaller than that of the leading edge. This makes the investigation of the effect of the leading edge sweep angle on the side force coefficient for the investigated 2.5D configuration of great interest.

When changing the sweep angle, the airfoil geometry in direction of the incoming flow is kept constant. The geometry perpendicular to the hinge-line or leading edge changes therefore between the configurations with differing sweep angle. In this direction the geometry is scaled by the cosine of the sweep angle. This means that the chord length perpendicular to the hinge-line increases with reduced sweep

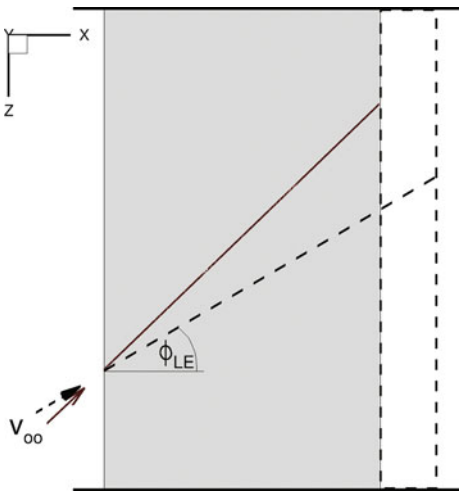

Fig. 5 Top view on the VTP section (stretched span) for two different sweep angles

angle and is the largest without any sweep. An example is shown in Fig. 5. Due to this, the area of the VTP section changes since the span is kept constant. Because of this, the respective area of the configuration A_{ref} is used when calculating the side force coefficient C_Y.

The leading edge sweep angle ϕ_{LE} is varied from 0° to 40° in 10°-steps. An additional result is the one of the configuration considered up to now with the 44° sweep angle. The slot configuration used is the one with $w = 9.6$ mm. For each leading edge sweep angle again the three blowing velocities are calculated as before.

Since the blowing direction of the jets is perpendicular to the hinge-line, the angle between them and the incoming flow is reduced with decreasing sweep angle. This has an influence on the vortex system generated over the rudder.

In Fig. 6 the increment of C_Y is shown which is the side force coefficient with the blowing jets activated from which the result of the same sweep angle configuration without blowing is subtracted. On the horizontal axis the momentum coefficient is depicted which varies with the sweep angle for the same blowing velocity due to the change in the reference area.

With increasing jet velocity at a constant sweep angle the side force coefficient is increased. The convergence of C_Y is without oscillations except for two cases with a sweep angle of 20° with jet velocities of 207 m/s and 239 m/s. Here the mean value and the amplitude are constant and the mean value is taken.

From the results it can be concluded that the sweep angle has a large effect on the side force increment which can be obtained by tangential blowing. One result is that a sweep angle of 30° leads to the highest increase in the side force coefficient as depicted in Fig. 6. Increasing the sweep angle reduces C_Y but reducing the sweep angle by the same amount leads to an even larger reduction in C_Y. Hence, the angle of the incoming flow to the blowing direction of the jets is quite important when designing such a tangential blowing AFC system.

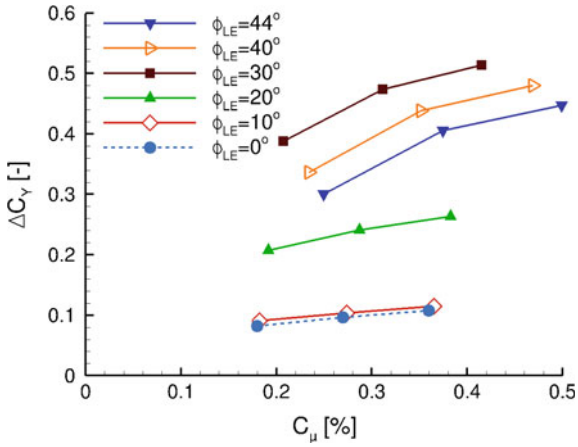

Fig. 6 C_Y increment versus C_μ for different sweep angle with each row showing results for three different jet velocities

To understand the results better, regions with negative skin friction coefficient C_{fx} are examined which give an indication of reversed and separated flow. This is done here exemplarily for the middle jet velocity of 207 m/s. Results are presented in Fig. 7. For the highest sweep angle of 44° the flow on the rudder can be attached up to the trailing edge. Just close to the rudder shoulder areas of reversed flow can be found. Here the vortices are not yet developed between the jets. For the other jet velocities the results are in principle similar. With decreased jet velocity of 169 m/s the separation areas increase while they decrease for the higher jet velocity of 239 m/s. A regular pattern of vortices for each slot similar to that in Fig. 4 is produced as is indicated by the regular running streamtraces in Fig. 7. The behavior for all adjacent jets is the same being deflected in the same direction. For the sweep angle of 40° and 30° the results are comparable.

The flow field on the rudder changes when decreasing the sweep angle further to 20°. Here also the decrease in C_Y could be observed before. Areas of separated flow from the rudder shoulder down to the trailing edge exist between the jets, although each individual jet can create a narrow band of attached flow up to the trailing edge. However, the area of separated flow on the rudder is quite large. It can be observed that with the angle between incoming flow and jet becoming smaller the vortex system gets more irregular and might indicate some unsteadiness which can not be captured by this steady calculation performed here. Some adjacent jets cluster, leaving between them larger areas in spanwise direction where separated flow regions can be found. This reduces the possible side force coefficient created there. The areas of separated flow increase for the even smaller sweep angles of 10° and 0°.

The more evenly distributed vortices for the higher sweep angle configurations are therefore preferable. Here the 30° configuration is the most effective one because the vortices are larger than those for the higher sweep angles covering a larger extent of the span.

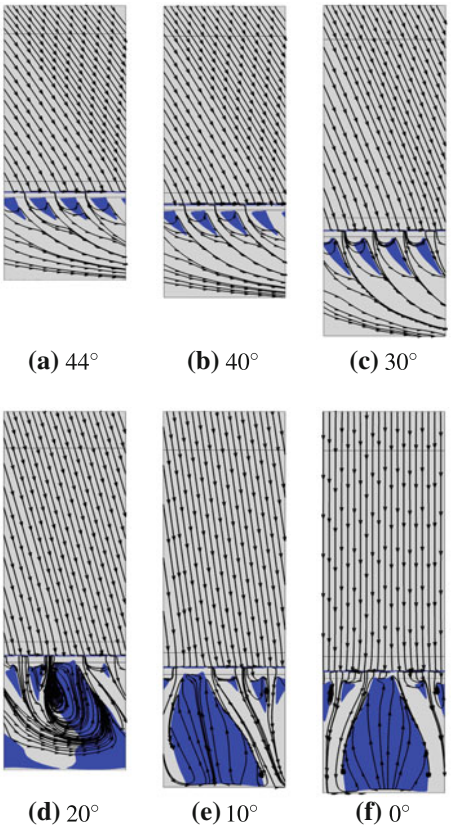

Fig. 7 Top view of the VTP section: Surface stream traces and areas marked with $C_{fx} < 0$ for different leading edge sweep angle ϕ_{LE}, $v_j = 207\,\mathrm{m/s}$

5.3 *Variation of Rudder Shoulder Curvature*

Two different approaches to construct the rudder were used. The first results presented in Sect. 5.1 were obtained with a larger radius of the rudder nose. Figure 8 shows a slice through the VTP section in direction of the incoming flow with 44° sweep. The results for the sweep angle variation were obtained using the second geometry with a smaller radius of the rudder shoulder and thus a higher curvature.

In Fig. 9 the effect on C_Y is shown. The values are all related to the result of the configuration without blowing for the initial airfoil. The smaller radius with the

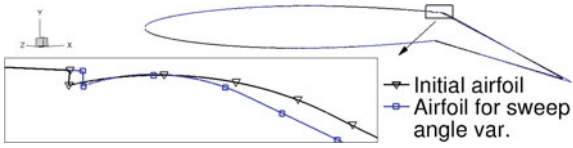

Fig. 8 Comparison of two airfoils with varying curvature of the rudder shoulder

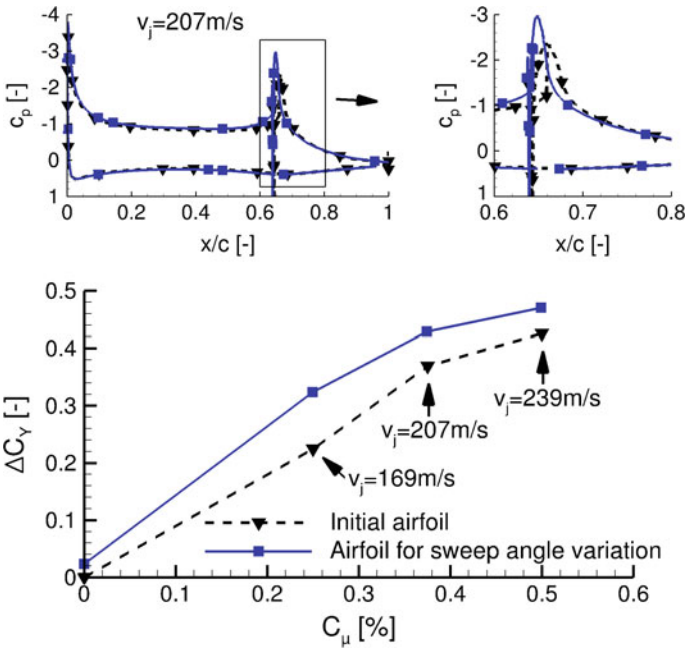

Fig. 9 C_Y increment versus C_μ for two different rudder nose curvature geometries incl. a pressure coefficient (c_p) distribution for $v_j = 207$ m/s (*top*)

higher curvature leads to an increase of the side force coefficient already without blowing. For the smallest blowing velocity the largest increment is obtained between the two geometries. For higher jet velocities the geometry with the higher curvature used for the sweep angle variation still leads to a higher C_Y of about 4% for $C_\mu = 0.5\%$. Due to the increased curvature the flow is more accelerated at the rudder shoulder, leading to a higher rudder suction peak there (cf. Fig. 9 top). This in turn also has an upstream effect on the fin where a small additional decrease in the pressure on the suction side is obtained. So in summary the radius of the rudder shoulder can have an observable influence on the gain in C_Y. When trying to adapt this kind of AFC technology to an aircraft it is, however, most probably that this radius is prescribed by other demands like mechanical functionality issues when rotating the rudder or by cruise shape requirements.

6 Summary

A numerical study is conducted where tangential blowing over the rudder shoulder of a 2.5D vertical tailplane with deflected rudder is investigated. Without blowing the flow over the rudder is separated. Blowing from a continuous slot extending over the

whole span is able to attach the flow on the rudder if a sufficiently high mass flow rate is applied. Using four discrete slots instead of a continuous one shows that a similar side force coefficient C_Y can be reached even with a reduction of the momentum coefficient by 50%. This large effect is based on the creation of a vortex pair at each finite jet which has a beneficial effect on the flow field over the rudder.

The development of this vortex pair is dependent on the angle of the incoming flow to the jet. First, the sweep angle of the leading edge of a VTP is used which is about 44°. This sweep angle is then gradually reduced. A sweep angle of 30° leads to the largest increase in the side force coefficient for the jet velocities considered. Since the hinge-line sweep angle of a 3D VTP is usually smaller than that of the leading edge this result seems to confirm that blowing perpendicular to the hinge-line is a quite good approach. In addition, the radius of the rudder shoulder has an influence on the obtainable side force coefficient. The geometry with the smaller radius leads here to an increase in C_Y. However, it is most likely that this parameter will be dictated by other constraints such as cruise shape or rudder deflection mechanical functionality requirements.

References

1. Burnazzi, M., Radespiel, R.: Design of a Droopnose Configuration for a Coanda Active Flap Application, AIAA Paper 2013-0487 (2013)
2. Centaursoft: Centaur Hybrid Grid Generation System Homepage. http://www.centaursoft.com. Cited 20 Sept 2016
3. Ciobaca, V.: Validation of Numerical Simulations for Separation Control on High-Lift Configurations. Ph.D. thesis, Forschungsbericht 2014-11, DLR (German Aerospace Center) (2014)
4. Gerhold, T.: Overview of the Hybrid RANS Code TAU. In: Kroll, N., Fassbender, J. (eds.) Notes on Numerical Fluid Mechanics and Multidisciplinary Design, MEGAFLOW—Numerical Flow Simulation for Aircraft Design, pp. 81–92. Springer, Heidelberg (2005)
5. Kröhnert, A.: Numerical investigation of tangential blowing at the rudder of a vertical Tailplane Airfoil. In: AIAA Paper 2014-2143, AIAA Aviation, Atlanta, Georgia (2014)
6. Lin, J.C., Andino, M.Y., Alexander, M.G., Whalen, E.A., Spoor, M.A., Tran, J.T., Wygnanski, I.J.: An Overview of Active Flow Control Enhanced Vertical Tail Technology Development, AIAA Paper 2016-0056 (2016)
7. Pfingsten, K.-C., Jensch, C., Körber, K.W., Radespiel, R.: Numerical simulation of the flow around circulation control airfoils. In: CEAS-2007-377, First CEAS European Air and Space Conference, Berlin (2007)
8. Pfingsten, K.C., Radespiel, R.: Experimental and numerical investigation of a circulation control airfoil. AIAA Paper 2009-533, Orlando, Florida (2009)
9. Shur, M.L., Strelets, M.K., Travin, A.K., Spalart, P.R.: Turbulence modeling in rotating and curved channels: assessing the spalart-shur correction. AIAA J. **38**(5), 784–792 (2000)
10. Spalart, P.R., Allmaras, S.R.: A One-Equation Turbulence Model for Aerodynamic Flows. AIAA Paper 92-0439, Reno, Nevada (1992)

Steady and Unsteady Numerical Simulation of a Bent Intake Geometry

Thomas Kächele, Tim Schneider and Reinhard Niehuis

Abstract A broad range of numerical flow simulations are carried out during the design phase of a highly bent intake geometry. The main aim is to evaluate the aerodynamic characteristics of a projected wind tunnel model and an estimation of mechanical loads for the structural dimensioning. The numerical setup using the TRACE code is validated first against comprehensive experimental data of a NASA s-duct test case. Three different turbulence models are found to be capable of reproducing the main flow features that occur in bent intake ducts with an acceptable accuracy. The following steady simulations of the symmetric wind tunnel model show asymmetric flow solutions and convergence problems for two of the three turbulence models. URANS computations are therefore carried out including a sensitivity study towards time-step size and domain volume. The unsteady results using the three different turbulence models still exhibit significant deviations concerning mechanical loads and duct performance. A safety margin is thus estimated from the unsteady data to be used for the construction and testing of the wind tunnel model.

1 Introduction

Modern aircraft concepts feature complex engine intake configurations for various reasons. The reduction of aircraft drag through boundary layer ingestion motivates the development of such civil configurations, a low observability by means of hiding the highly reflective fan plane of the jet engine lies in the focus of military applications. These unconventional intake geometries result in a disturbed flow regime towards the compression system of the jet engine. The consequences are

T. Kächele (✉) · R. Niehuis
Institute of Jet Propulsion, Universität der Bundeswehr München,
Werner-Heisenberg-Weg 39, 85577 Neubiberg, Germany
e-mail: thomas.kaechele@unibw.de

T. Schneider
MTU Aero Engines AG, Dachauer Str. 665, 80995 Munich, Germany
e-mail: Tim.Schneider@mtu.de

A. Dillmann et al. (eds.), *New Results in Numerical and Experimental Fluid Mechanics XI*, Notes on Numerical Fluid Mechanics and Multidisciplinary Design 136, https://doi.org/10.1007/978-3-319-64519-3_2

performance deficits and a reduced stability margin. The generated flow distortion within the aerodynamic interface plane (AIP) between intake and engine is both dependent on the duct geometry as well as the upstream influence of the compressor. In order to improve the knowledge about this interaction and to validate different simulation approaches, a highly bent intake geometry was developed for an experimental investigation in cooperation with MTU Aero Engines AG [1]. Experiments will take place in the engine test facility of the Institute of Jet Propulsion at the University of the German Federal Armed Forces in Munich featuring the MexJET test engine [2]. During the iterative design process, numerical flow simulations were carried out for two reasons. The first is the prediction and evaluation of the resulting distortion pattern to achieve a significant AIP flow distortion without the risk of compressor surge. The second reason is an estimation of the expected wall pressure distribution to simulate the mechanical loads on the duct as well as on the support structure. As the simulation of highly contoured intake geometries by means of RANS calculations is very challenging, an estimation of numerical uncertainness and thus an additional safety margin for the load cases was necessary.

2 Intake Aerodynamics

During the design phase of the duct, no best practice setup for the simulation of intake ducts with the flow solver TRACE was available. The numerical settings were therefore calibrated using comprehensive experimental data generated by a NASA test campaign of a comparable single s-bent duct by Wellborn and Okiishi [3]. This geometry is compared to the MexJET duct in Fig. 1. The NASA duct on the left side

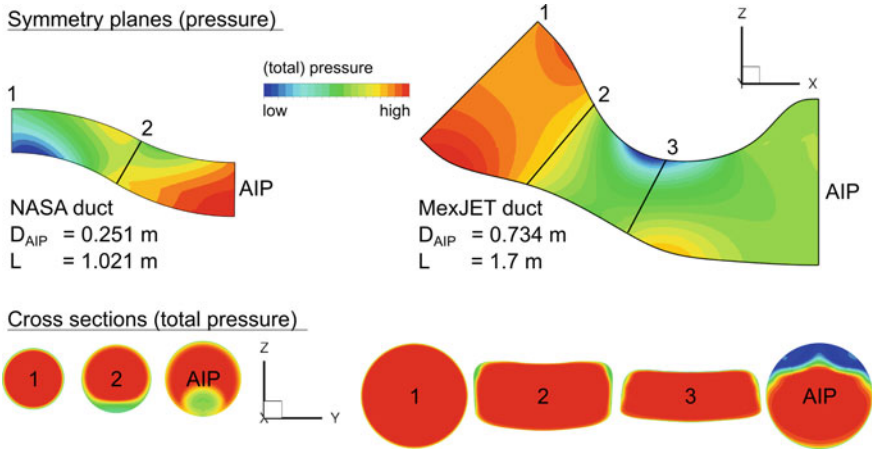

Fig. 1 Comparison of NASA duct (*left*) and MexJET duct (*right*) with pressure values in the symmetry plane and total pressure values in different cross sections in the same scale